

Thermodynamic Properties of Fermi Systems with Flat Single-Particle Spectra

V. A. Khodel,^{1,2} J. W. Clark,² and M. V. Zverev¹

¹ *Russian Research Centre Kurchatov Institute, Moscow, 123182, Russia*

² *McDonnell Center for the Space Sciences and Department of Physics,
Washington University, St. Louis, MO 63130, USA*

(Dated: September 13, 2018)

The behavior of strongly correlated Fermi systems is investigated beyond the onset of a phase transition where the single-particle spectrum $\xi(\mathbf{p})$ becomes flat. The Landau-Migdal quasiparticle picture is shown to remain applicable on the ordered side of this transition. Nevertheless, low-temperature properties evaluated within this picture show profound changes relative to results of Landau theory, as a direct consequence of the flattening of $\xi(\mathbf{p})$. Stability conditions for this class of systems are examined, and the nature of antiferromagnetic quantum phase transitions is elucidated.

PACS numbers: 71.10.Hf, 71.27.+a

Low-temperature properties of strongly correlated Fermi systems exhibit features not inherent in Landau Fermi liquids [1, 2, 3, 4, 5, 6, 7, 8, 9, 10]. Of special importance is the scaling behavior $\chi^{-1}(T, H) = \chi^{-1}(0, H) + T^\alpha F(H/T)$ of the inverse magnetic susceptibility, observed so far only in heavy fermion metals [5, 7, 8, 9, 10] in weak, sometimes tiny external magnetic fields H . This feature rules out the collective, spin-fluctuation scenario advanced in Refs. 11, 12 to explain the non-Fermi-liquid (NFL) behavior of these systems, while providing evidence for the direct relevance of single-particle degrees. Earlier work within this picture [13] has evaluated thermodynamic properties on the “metallic” side of a phase transition associated with the rearrangement of the Landau state in strongly correlated Fermi systems. Here we focus attention on the situation beyond the critical point where the Landau state becomes unstable.

This state is known (e.g. from Refs. 14, 15) to lose its stability at a density $n = n_b$ where a bifurcation point $p = p_b$ emerges in the equation

$$\xi(p, n, T = 0) = 0, \quad (1)$$

which ordinarily has only the single root $p = p_F$. (Here $\xi(p) = \varepsilon(p) - \mu$ is the single-particle energy measured from the chemical potential μ .) We shall focus on the case $|p_F - p_b| \ll p_F$, where the critical single-particle spectrum has the form

$$\xi(p, n_b, T = 0) \sim (p - p_b)^2(p - p_F). \quad (2)$$

Thus if p_b coincides with p_F , the effective mass $M^*(n)$ diverges at n_b ; in the general case $p_b \neq p_F$, the Landau state loses its stability before M^* becomes infinite. Beyond the critical density n_b , Eq. (1) possesses two additional roots p_1 and p_2 with $p_1 < p_b < p_2$. The spectrum $\xi_{FL}(p, T = 0)$, evaluated with the FL momentum distribution $n_{FL}(p) = \theta(p_F - p)$, then takes the form

$$\xi_{FL}(p, n, T = 0) \sim (p - p_1)(p - p_2)(p - p_F). \quad (3)$$

If $p_b \neq p_F$, the roots p_1, p_2 are both located either in the interior of the Fermi sphere or both outside it. If $p_b = p_F$, then $p_1 < p_F < p_2$. In all these cases, the occupation numbers $n_{FL}(p)$ are rearranged. As a rule, the Fermi surface becomes multi-connected, but at $T = 0$, the quasiparticle occupation numbers continue to take values 0 or 1. Hence the Landau-Migdal quasiparticle picture holds, with $n(\xi) = 1$ for $\xi < 0$ and 0 otherwise. Consider first the case $p_1 < p_2 < p_F$. Then according to Eq. (3), the single-particle states remain filled in the intervals $p < p_1$ and $p_2 < p < p_F$, while the states with $p_1 < p < p_2$ are empty. We call this new phase the bubble phase. If $p_b = p_F$, then $p_1 < p_F$ and $p_2 > p_F$, and the states with $p < p_1$ and with $p_F < p < p_2$ are occupied, while those for $p_1 < p < p_F$ are empty. Again one deals with the bubble phase.

At this point, we observe that the solution (3) is not self-consistent, since the spectrum is evaluated with $n_{FL}(p)$ while the true Fermi surface is doubly-connected. Following Ref. 14, we consider the feedback of the rearrangement of $n_{FL}(p)$ on the spectrum $\xi(p)$ in the bubble phase based on the Landau relation [16, 17]

$$\frac{\partial \varepsilon(p)}{\partial \mathbf{p}} = \frac{\mathbf{p}}{M} + \int f(\mathbf{p}, \mathbf{p}_1) \frac{\partial n(p_1)}{\partial \mathbf{p}_1} d\mathbf{p}_1, \quad (4)$$

where f is the scalar part of the Landau interaction function and $n(p) = [1 + \exp(\xi/T)]^{-1}$ is the quasiparticle momentum distribution. For the electron liquid within a solid, \mathbf{p}/M is to be replaced by $\partial \varepsilon_{\mathbf{p}}^0 / \partial \mathbf{p}$, where $\varepsilon_{\mathbf{p}}^0$ is the LDA electron spectrum. To date, Eq. (4) has been solved only in 3D Fermi systems with functions f depending on $q = |\mathbf{p} - \mathbf{p}_1|$. Despite the diversity of forms assumed for $f(q)$, the resulting spectra and momentum distributions bear a close family resemblance. This robustness is illustrated in Figs. 1 and 3, which display results [14] from solution of Eq. (4) for the interaction function

$$f(q) = \lambda_1 / [(q/p_F)^2 + \beta_1^2], \quad (5)$$

and in Figs. 2 and 4, which present results for

$$f(q) = \lambda_2 / [((q/2p_F)^2 - 1)^2 + \beta_2^2]. \quad (6)$$

How do the bubble solutions of Eq. (4) evolve under variation of T ? At extremely low $T < T_{FL} \sim (p_2 - p_1)^2/M$, these states are described by FL theory with the enhanced effective mass $M^* \sim Mp_F/(p_2 - p_1)$. Heating above T_{FL} results in their dissolution (see Figs. 1 and 2). With further increase of T , the spectrum $\xi(p)$ becomes smoother, and in the region of a new critical temperature T_Z , a flat portion $\xi \simeq 0$ appears over an interval $[p_i, p_f]$ surrounding the point p_F , as shown in the left panels of Figs. 3 and 4. The presence of this flat portion of $\xi(p)$ is a signature of the phenomenon called fermion condensation [18, 19, 20]. Since $\xi(p) = \varepsilon(p) - \mu$ and $\varepsilon(p) = \delta E_0/\delta n(p)$, the equality $\xi = 0$ can be rewritten as a variational condition

$$\frac{\delta E_0}{\delta n(p)} = \mu, \quad p_i < p < p_f, \quad (7)$$

with $E_0 = \sum_{\mathbf{p}} \varepsilon_{\mathbf{p}}^0 n(\mathbf{p}) + \frac{1}{2} \sum_{\mathbf{p}, \mathbf{p}_1} f(\mathbf{p} - \mathbf{p}_1) n(\mathbf{p}) n(\mathbf{p}_1)$ and $\varepsilon_{\mathbf{p}}^0 = p^2/2M$. The solution $n_0(p)$ of Eq. (4), or equivalently of Eq. (7), is a continuous function of p with a nonzero derivative dn_0/dp . The set of states with $\xi(p) = 0$ is called the fermion condensate (FC), since the associated density of states contains a Bose-liquid-like term $\eta n \delta(\varepsilon)$. The dimensionless constant $\eta \simeq (p_f - p_i)/p_F$ is identified as a characteristic parameter of the FC phase.

It has been shown [20] that the FC “plateau” in $\xi(p)$ has a small slope, evaluated by inserting $n_0(p)$ into the above Fermi-Dirac formula for $n(\xi)$ to yield

$$\xi(p, T \geq T_Z) = T \ln \frac{1 - n_0(p)}{n_0(p)}, \quad p_i < p < p_f. \quad (8)$$

As indicated in the bottom-right panels of Figs. 3 and 4, at $T \geq T_Z$ the ratio $\xi(p)/T$ is indeed a T -independent function of p in the FC region. The width $\xi(p_f) - \xi(p_i) \equiv \xi_f - \xi_i$ of the FC “band” appears to be of order T , almost independently of $\eta > \eta_{\min} \sim 10^{-2}$. Thus at $\eta > \eta_{\min}$ the FC group velocity is estimated as

$$\left(\frac{d\xi(p, T)}{dp} \right)_T \sim \frac{T}{\eta p_F}, \quad p_i < p < p_f. \quad (9)$$

Outside the FC domain, $\xi(p)$ still remains flat (see Figs. 3, 4), and contributions to thermodynamic properties from the regions adjacent to p_i and p_f also play significant roles in their NFL behavior. Indeed, consider for example the static magnetic susceptibility

$$\chi(T) = -\mu_B^2 \Pi_0(\omega = 0) [1 - g_0 \Pi_0(\omega = 0)]^{-1}. \quad (10)$$

Here μ_B denotes the Bohr magneton [21] and g_0 the zeroth harmonic of the spin-spin interaction function, while $\Pi_0(\omega = 0) = \int (dn(\xi)/d\xi) dv$ is the static particle-hole propagator.

The propagator $\Pi_0(\omega = 0) \equiv -N_0(P_f(T) + P_n(T))/T$, where N_0 is the density of states of the ideal Fermi gas,

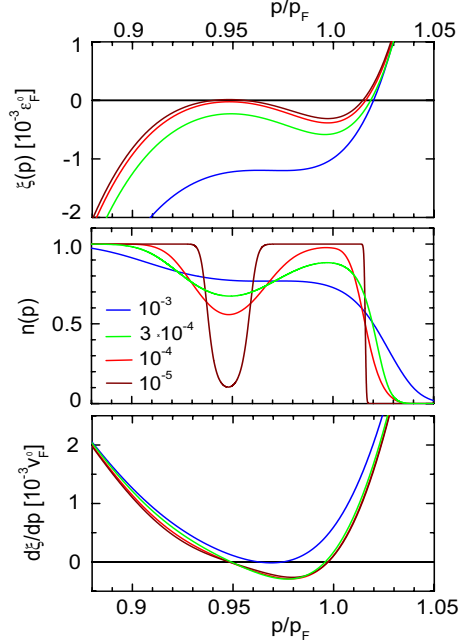


FIG. 1: Single-particle spectrum $\xi(p)$ in units of $10^{-3} \varepsilon_F^0$, where $\varepsilon_F^0 = p_F^2/2M$ (top panel), occupation numbers $n(p)$ (middle panel), and $d\xi/dp$ in units of $10^{-3} v_F^0$, where $v_F^0 = p_F/M$ (bottom panel), plotted versus p/p_F at four color-coded temperatures relevant to the bubble phase, in units of ε_F^0 . The model (5) is assumed with parameters $\beta_1 = 0.07$ and $\lambda_1 = 0.45 N_0$, where $N_0 = p_F M/\pi^2$.

is the sum of a FC part given by

$$P_f(T) = \frac{1}{p_F} \int_{p_i}^{p_f} n_0(p) [1 - n_0(p)] dp \sim \eta \quad (11)$$

and a noncondensate part $P_n(T) \equiv P_n^>(T) + P_n^<(T)$ consisting of two terms. Defining

$$P_n(T; \xi_1, \xi_2) = \frac{1}{p_F} \int_{\xi_1}^{\xi_2} \frac{n(\xi) [1 - n(\xi)] d\xi}{(d\xi/dp)}, \quad (12)$$

the two terms become $P_n^< = P_n(T; -\mu, \xi_i)$ and $P_n^> = P_n(T; \xi_f, \infty)$. According to Eq. (2), at small η one has

$$d\xi(p \rightarrow p_f)/dp = v_f(T) + v_2(p - p_f)^{s-1} + \dots, \quad (13)$$

with $v_f(T) \sim T$ (see Eq. (9)) and $s = 2$ and 3 , respectively, for the cases $p_b \neq p_F$ and $p_b = p_F$. An analogous formula applies for the group velocity $d\xi/dp$ outside the FC domain close to the point p_i . Based on these results, algebra similar to that performed in Ref. 13 leads to

$$\Pi_0(\omega = 0) = -N_0 \tau^{-1} [P_f \eta + P_n \tau^{1/s}] + \text{const}, \quad (14)$$

where $\tau = T/\varepsilon_F^0$ is the dimensionless temperature.

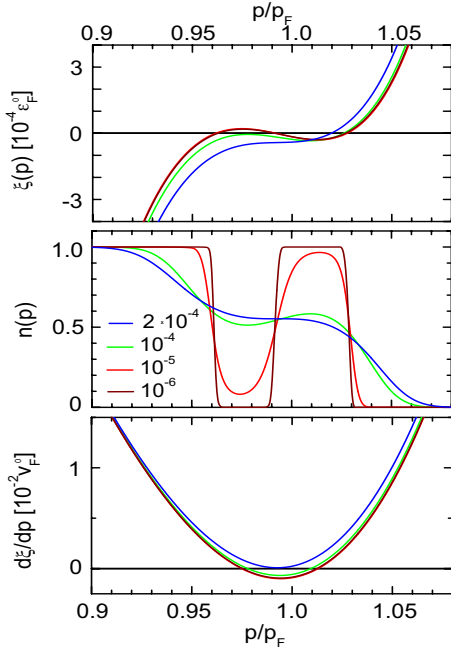


FIG. 2: Same as in Fig. 1 but for the model (6) with parameters $\lambda_2 = 3 N_0$ and $\beta_2 = 0.48$.

The NFL excess $\Delta\chi(T, \rho) = \chi(T, \rho) - \chi_{FL}(\rho)$ over the Pauli result then acquires the form

$$\Delta\chi(T, \rho) \sim \mu_B^2 N_0 \tau^{-1} \frac{P_f \eta + P_n \tau^{1/s}}{1 + g_0(\rho) N_0 \tau^{-1} (P_f \eta + P_n \tau^{1/s})}. \quad (15)$$

We see that at small $\eta < \tau^{1/s}$ the FC plays a minor role, and the NFL part of χ behaves as

$$\chi(T) \sim T^{-1+1/s}. \quad (16)$$

By contrast, in the case $\eta > \tau^{1/s}$ the FC contribution to Eq. (15) is predominant, and the magnetic susceptibility mimics that of a gas of localized spins

$$\chi(T) \sim (T - \Theta_W)^{-1}, \quad (17)$$

with the Weiss temperature $\Theta_W \simeq -g_0 \eta(\rho) \rho$.

In heavy-fermion metals, both index regimes, i.e. $s = 2$ [4] and $s = 3$ [7], are present, while data on the magnetic susceptibility of 2D liquid ^3He are compatible only with $s = 3$. Fig. 5 compares results from Eq. (15) for 2D liquid ^3He with experimental data of Ref. 1 at the densities $\rho = 0.052 \text{ \AA}$ and $\rho = 0.058 \text{ \AA}$. We have made these parameter choices: $P_n = 0.2$, $P_f = 1$, $\eta = 0$ (lower curve), and $\eta = 0.04$ (upper curve). The theoretical results are seen to be in agreement with the experimental data.

The FC contributions to other thermodynamic properties are found by inserting the distribution $n_0(p)$ into the corresponding Landau formulas. In particular, the FC entropy S_f arising at $T \simeq T_Z$ is $S_f = -\sum [n_0(p) \ln n_0(p) + (1 - n_0(p)) \ln(1 - n_0(p))] \sim \eta$. This

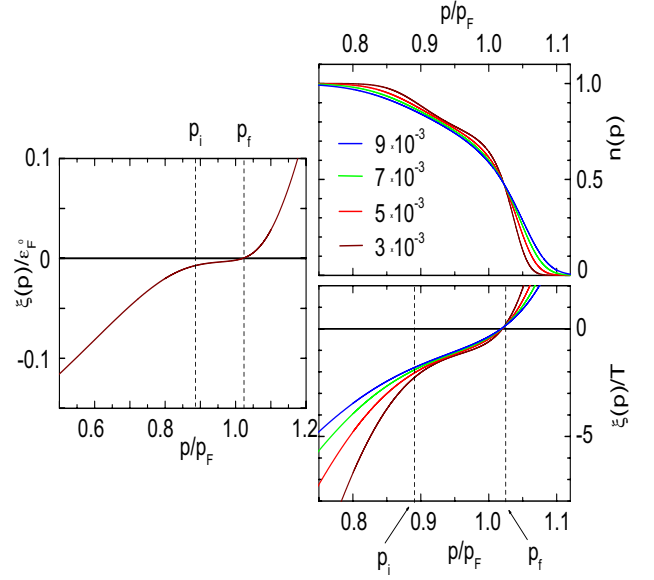


FIG. 3: Single-particle spectrum $\xi(p)$ in units of ε_F^0 at the critical temperature $T_Z = 3 \times 10^{-3} \varepsilon_F^0$ (left panel), occupation numbers $n(p)$ (right-top panel), and $\xi(p)/T$ (right-bottom panel), plotted versus p/p_F at four color-coded temperatures relevant to the phase with a fermion condensate, in units of ε_F^0 . The model (5) is assumed.

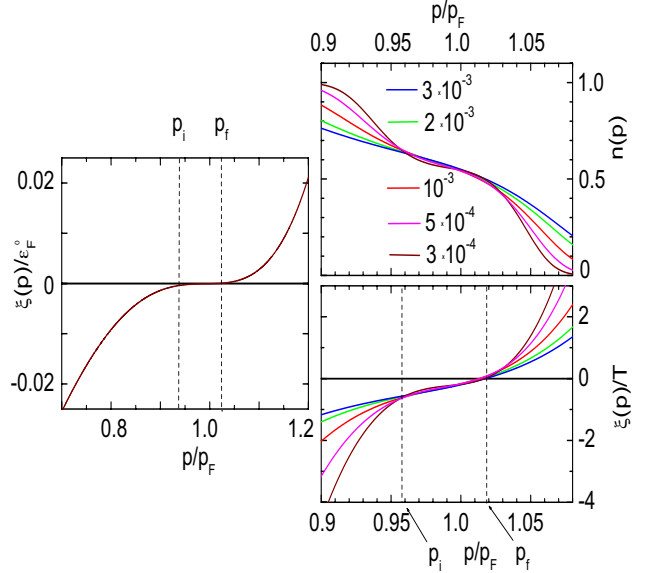


FIG. 4: Same as in Fig. 3 but for the model (6). The single-particle spectrum in the left panel is shown at $T_Z = 3 \times 10^{-4} \varepsilon_F^0$.

term does not contribute to the specific heat $C(T) = T \partial S(T, \rho) / \partial T$; however, it does affect the thermal expansion $\beta(T) \sim \partial S(T, \rho) / \partial \rho$ [22], giving rise to a great enhancement of the Grüneisen ratio $\beta(T)/C(T)$, observed at low T in several heavy-fermion metals [7, 23].

Our analysis has been carried out within the Landau-

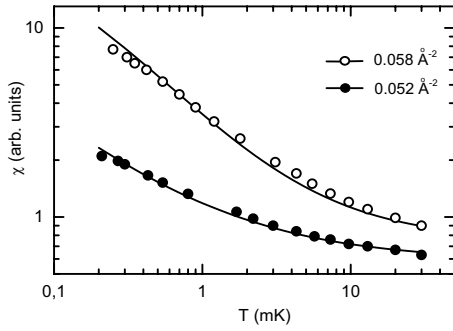


FIG. 5: Low-temperature magnetic susceptibility of ^3He films. Experimental data from Ref. 1 appear as solid and open circles and solid squares, while solid curves trace the predictions of the current theory at low T .

Migdal quasiparticle picture where damping γ of single-particle excitations is neglected. It is applicable to systems containing a FC, provided the dimensionless damping rate $\gamma(T)/T$ remains small at $T \sim T_Z$. To establish this property, we adopt the standard formula [17]

$$\gamma(\varepsilon \sim T) \sim \sum_{\mathbf{q}} \int_0^{\varepsilon \sim T} |\Gamma^2(q, \omega)| \text{Im} \Pi_0(\mathbf{q}, \omega) \text{Im} G_R(\mathbf{p} - \mathbf{q}, \omega - \varepsilon) d\omega, \quad (18)$$

Γ being the scattering amplitude and $G_R(p, \varepsilon)$ the retarded Green function. With a FC present, overwhelming contributions to the collision term (18) are known to come from a region $q < q_c = \eta p_F$ where $\text{Im} \Pi_0(\mathbf{q}, \omega)$ substantially exceeds the ideal-Fermi-gas value [20]. Factoring out $|\Gamma|^2$ from the integral (18), a straightforward argument [20] yields $\gamma(T) \sim T^{-1}$. However, this treatment is erroneous, since it misses the suppression of the integral (18) stemming from the inequality $|\Gamma(q, \omega)| < [\text{Im} \Pi_0(q, \omega)]^{-1}$ [25]. Upon inserting this inequality into Eq. (18) we are led to the result

$$\gamma(T) < \int_{q < q_c} \int_0^T \frac{\text{Im} G_R(\mathbf{p} + \mathbf{q}, \varepsilon + \omega)}{|\text{Im} \Pi_0(q, \omega \sim T)|} d\mathbf{q} d\omega. \quad (19)$$

In the 2D electron gas this formula coincides with that derived in Ref. [26]. Based on Eq. (19), the putative behavior $\gamma(T) \sim T^{-1}$ is replaced by

$$\gamma(T) \sim T \eta \ln(1/\eta). \quad (20)$$

In deriving this result, we have taken account of the fact that in the system with a FC, the Fermi velocity $v_F = p_F/M^*$ entering the corresponding expression for $\gamma(T)$ in Ref. [26] must be replaced by the FC group velocity $(d\xi/dp)_T = T/\eta p_F$. (More details may be found in Ref. [24].) Similar results are obtained in the 3D case, but without the logarithmic correction $\ln(1/\eta)$. We conclude that the quasiparticle picture holds in systems with a FC, at least when $\eta \ll 1$.

Finally, we consider stability conditions for systems with a flat portion in the spectrum $\xi(p)$. To be definite, we examine the spin-density wave channel and suppose that at the critical density n_b , the associated stability condition, which has the form

$$1 > g_0(k_c) \Pi_0(k_c, \omega=0) \equiv g_0(k_c) \int \frac{n(\mathbf{p}) - n(\mathbf{p} + \mathbf{k}_c)}{\xi(\mathbf{p}) - \xi(\mathbf{p} + \mathbf{k}_c)} dv, \quad (21)$$

is not yet violated. Beyond the density n_b , the magnitude of the NFL component of Π_0 , proportional to η , drops rapidly with increasing T (see e.g. Eq. (14)). In the present case this implies that violation of the inequality (21) can occur only at very low T . Furthermore, numerical calculations show that in systems with a FC, the NFL part of the function $\Pi_0(k, \omega=0)$ has a maximum at small nonzero $k \leq \eta p_F$; one expects a new ground state possessing a long-range magnetic superstructure, as well as a small ordered magnetic moment. A salient feature revealed in Refs. [13, 27, 28] is the destruction of the flat portion of the spectrum $\xi(p)$ by imposition of sufficiently weak magnetic fields, which also kills the magnetic ordering. Such a quantum phase transition has been uncovered in recent experiments on YbAgGe [29]. The interplay between quantum antiferromagnetism built upon a FC, and the FC itself, will be the subject of a future article.

The present investigation has revealed generic features of strongly interacting Fermi systems which exhibit a flat single-particle spectrum $\xi(p)$. We have shown that the quasiparticle picture remains applicable in the evaluation of thermodynamic properties of such systems, and that the flattening of $\xi(p)$ is a principal source of their non-Fermi-liquid behavior.

We thank V. V. Borisov, P. Coleman, V. M. Galitski, V. G. Orlov, and V. M. Yakovenko for valuable discussions. This research was supported by NSF Grant PHY-0140316 (JWC and VAK), by the McDonnell Center for the Space Sciences (VAK), and by the Grant NS-1885.2003.2 from the Russian Ministry of Education and Science (VAK and MVZ).

-
- [1] C. Bäuerle *et al.*, J. Low Temp. Phys. **110**, 333 (1998).
 - [2] M. Morishita, H. Nagatani, and H. Fukuyama, J. Low Temp. Phys. **113**, 299 (1998).
 - [3] A. Casey, H. Patel, J. Nyéki, B. P. Cowan, and J. Saunders, Phys. Rev. Lett. **90**, 115301 (2003).
 - [4] H. V. Löhneysen *et al.*, Phys. Rev. Lett. **72**, 3262 (1994).
 - [5] A. Schröder *et al.*, Nature **407**, 351 (2000).
 - [6] G. R. Stewart, Rev. Mod. Phys. **73**, 787 (2001).
 - [7] R. Küchler *et al.*, Phys. Rev. Lett. **91**, 066405 (2003).
 - [8] D. Takahashi *et al.*, Phys. Rev. B **67**, 180407(R) (2003).
 - [9] P. Gegenwart *et al.*, Acta Phys. Pol. B **34**, 323 (2003).
 - [10] J. Custers *et al.*, Nature **424**, 524 (2003).
 - [11] J. A. Hertz, Phys. Rev. B **14**, 1165 (1976).
 - [12] A. J. Millis, Phys. Rev. B **48** 7183 (1993).

- [13] J. W. Clark, V. A. Khodel, and M. V. Zverev, Phys. Rev. B **71**, 012401 (2005).
- [14] M. V. Zverev and M. Baldo, JETP **87**, 1129, (1998); J. Phys. Condens. Matter **11**, 2059 (1999).
- [15] M. Baldo *et al.*, J. Phys. Condens. Matter **16**, 6431 (2004).
- [16] L. D. Landau and E. M. Lifshitz, *Statistical physics*, Vol. 2 (Pergamon Press, Oxford, 1980).
- [17] A. A. Abrikosov, L. P. Gor'kov, and I. E. Dzyaloshinski, *Methods of Quantum Field Theory in Statistical Physics* (London, Prentice-Hall, 1963).
- [18] V. A. Khodel and V. R. Shaginyan, JETP Letters **51**, 553 (1990); Condensed Matter Theories **12**, 221 (1997).
- [19] G. E. Volovik, JETP Letters **53**, 222 (1991).
- [20] P. Nozières, J. Phys. I France **2**, 443 (1992).
- [21] In heavy-fermion metals, plane waves are replaced by Bloch waves and μ_B by μ_{eff} .
- [22] M. V. Zverev, V. A. Khodel, V. R. Shaginyan and M. Baldo, JETP Lett. **65**, 863 (1997).
- [23] R. K  chler *et al.*, Phys. Rev. Lett. **93**, 096402 (2004).
- [24] V. A. Khodel, J. W. Clark, and M. V. Zverev, cond-mat/0501427.
- [25] V. A. Khodel and P. Schuck, Z. Phys. B **104**, 503 (1997).
- [26] G. F. Giuliani and J. J. Quinn, Phys. Rev. B **26**, 4421 (1982).
- [27] V. R. Shaginyan, JETP Letters **79**, 286 (2004)
- [28] M. V. Zverev and V. A. Khodel, JETP Letters **79**, 635 (2004).
- [29] B. F  k *et al.*, cond-mat/04107361.